

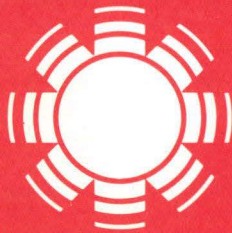
SERI/TR-631-602

July 1981

Optical Analysis and Optimization of Parabolic Trough Collectors

A User's Guide

P. Bendt
A. Rabl
H. W. Gaul



SERI

Solar Energy Research Institute

A Division of Midwest Research Institute

1617 Cole Boulevard
Golden, Colorado 80401

Operated for the
U.S. Department of Energy
under Contract No. EG-77-C-01-4042

SERI/TR-631-602

c.2

Printed in the United States of America
Available from:
National Technical Information Service
U.S. Department of Commerce
5285 Port Royal Road
Springfield, VA 22161
Price:
Microfiche \$3.00
Printed Copy \$4.50

NOTICE

This report was prepared as an account of work sponsored by the United States Government. Neither the United States nor the United States Department of Energy, nor any of their employees, nor any of their contractors, subcontractors, or their employees, makes any warranty, express or implied, or assumes any legal liability or responsibility for the accuracy, completeness or usefulness of any information, apparatus, product or process disclosed, or represents that its use would not infringe privately owned rights.

SERI/TR-631-602
UC CATEGORY: 62a,b,e

SOLAR ENERGY RESEARCH INSTITUTE
Solar Energy Information Center

OCT 2 1981

GOLDEN, COLORADO 80401

OPTICAL ANALYSIS AND OPTIMIZATION
OF PARABOLIC TROUGH COLLECTORS

A USER'S GUIDE

P. BENDT
A. RABL
H. W. GAUL

JULY 1981

PREPARED UNDER TASK NO. 3432.30

Solar Energy Research Institute

A Division of Midwest Research Institute

1617 Cole Boulevard
Golden, Colorado 80401

Prepared for the
U.S. Department of Energy
Contract No. EG-77-C-01-4042

SERI report

FOREWORD

This is a user's guide, based on the SERI report TR-34-092 titled "Optical Analysis and Optimization of Line Focus Solar Collectors" by P. Bendt, A. Rabi, H. W. Gaul, and K. A. Reed (Sept. 1979). It was prepared under Contract No. EG-77-C-01-4047 and SERI Task No. 3432.30. The authors thank F. Kreith for many helpful comments.



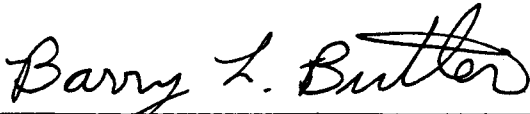
Ari Rabi

Approved for

SOLAR ENERGY RESEARCH INSTITUTE



Frank Kreith, Branch Chief
Solar Thermal Research



Barry L. Butler, Division Manager
Solar Thermal, Ocean, & Wind Division

ABSTRACT

The results of a detailed optical analysis of parabolic trough solar collectors are summarized by a few universal graphs and curve fits. These graphs enable the designer of parabolic trough collectors to calculate the performance and optimize the design with a simple hand calculator. The method is illustrated by specific examples that are typical of practical applications. The sensitivity of the optimization to changes in collector parameters and operating conditions is evaluated.

TABLE OF CONTENTS

	<u>Page</u>
1.0 Introduction.....	1
2.0 Optimization Philosophy.....	3
3.0 Collector Parameters.....	5
4.0 Choice of Rim Angle.....	9
5.0 Optimization of Concentration Ratio.....	11
6.0 Calculation of Intercept Factor and Operating Efficiency.....	15
7.0 Sensitivity of Optimization to Changes in Collector Parameters.....	19
8.0 Operation with North-South Axis.....	21
9.0 References.....	23

LIST OF FIGURES

	<u>Page</u>
1 (a) Heat Loss Coefficient vs. Gap Size; (b) Heat Loss Coefficient Variance with Absorber Diameter; (c) Heat Loss Coefficient vs. Temperature.....	8
2 Intercept Factor γ vs. Rim Angle ϕ for Parabolic Trough (a) with Cylindrical Receiver (b) with Flat Receiver.....	9
3 The Curve G ($\sigma_{tot}C$) for Finding the Optimal Concentration Ratio for Different Rim Angles ϕ for (a) a Cylindrical Receiver (b) a Flat Receiver.....	14
4 Intercept Factor γ vs. $\sigma_{tot}C$ for Different Rim Angles ϕ (Gaussian Approximation) for (a) a Cylindrical Receiver (b) a Flat Receiver.....	16

LIST OF TABLES

1 Collector Parameters.....	5
2 Tracking Modes and Associated Solar Data.....	11
3 Worksheet for Optimization of Concentration Ratio for Parabolic Trough with East-West Axis.....	12
4 Quantities Needed for Evaluation of Transverse Effects of Longitudinal Contour Errors in Parabolic Trough with East-West Tracking Axis.....	13
5 Worksheet for Calculation of Efficiency for Collector Optimized According to Table 3.....	16
6 Sensitivity of Optimization to Change in Heat Loss Parameter q_L	19
7 Calculation of Efficiency of Collector with $C = 27.3$ (Optimized for East-West Axis) If Operated with Horizontal North-South Axis.....	21

NOMENCLATURE

The optimization procedure proposed in this paper is based on typical all-day average values of insolation. All-day averages are designated by angular brackets $\langle \rangle$. Subscripts \parallel and \perp designate angular variables measured parallel or transverse to the tracking axis.

Glossary:

Concentration ratio	Ratio of aperture area over receiver surface area. For example, a trough of aperture width D and receiver tube diameter d has $C = D/(\pi d)$.
Rim angle	Angle between symmetry axis of parabola and line from focus to edge of parabolic reflector
C	Geometric concentration ratio
C_o	Optimal concentration ratio
D	Aperture width
d	Absorber diameter
I_b	Beam component of solar irradiance (W/m^2) as measured by pyrheliometer (also known as direct normal insolation)
$\langle I_b \cos \theta \rangle$	Day-long average beam irradiance on collector aperture (including cosine factor)
I_d	Diffuse component of solar irradiance, assumed to be isotropic (W/m^2)
I_h	Hemispherical irradiance on horizontal surface
I_{in}	Portion of I_b that would reach the receiver if $(\rho\tau\alpha)$ were equal to 1
q_L	Cq_{loss} = heat loss in W per m^2 of receiver surface area
q_{loss}	Heat loss per aperture area
q_{net}	Power output of collector (W/m^2 of aperture area)
U_L	Heat loss coefficient ($W/m^2\text{ }^\circ C$) based on receiver surface area
X	$X_S + \left(\frac{q_L}{(\rho\tau\alpha)} - I_d \right) / I_b$ = critical intensity ratio
X_S	Contribution of shading term to critical intensity ratio
α	Absorptance of receiver
γ	I_{in}/I_b = intercept factor
δ	Declination
η	q_{net}/I_b = collector efficiency

NOMENCLATURE (concluded)

η_o	Optical efficiency = $(\rho\tau\alpha)\gamma$
θ	Incidence angle
$\lambda(\theta)$	Factor accounting for rim-angle-dependent contribution of longitudinal mirror errors to transverse beam spreading
$(\rho\tau\alpha)$	Effective reflectance-transmittance-absorptance product of collector
σ_{contour}	rms angular deviation of contour from design direction
$\sigma_{\text{displacement}}$	Equivalent rms angular spread that accounts for imperfect placement of receiver
σ_{optical}	rms angular spread caused by all optical errors
σ_{specular}	rms spread of reflected beam due to imperfect specularity of reflector material
s_{sun}	rms angular width of sun in line focus geometry
σ_{tot}	Total rms beam spread
σ_{tracking}	rms tracking error
τ	Transmittance of collector glazing
θ	Rim angle
θ_o	Optimal rim angle

SECTION 1.0

INTRODUCTION

The optical analysis of solar collectors with parabolic reflectors must take into account many different effects, such as the finite size of the sun, aberrations at nonnormal incidence, as well as errors in surface contour, receiver placement and tracking. The calculations are so complicated that most previous investigations [1-3] have resorted to computer simulation. Such purely numerical approaches can provide an enormous amount of detailed information, but they obscure functional relationships and intuitive understanding. The results of these investigations were not sufficiently transparent to serve as design guides, and the guides that have been available so far are rather limited in scope. Singh and Cheema [4], for example, do not calculate the amount of insolation intercepted by the receiver, and Treadwell [3] considers only a narrow range of collector parameters and operating conditions.

This paper is based on an analytical solution [5] that is more amenable to developing a design guide. By identifying the important functional relationships we have been able to summarize the results of the optical analysis with a few universal graphs and curve fits. The details of the analysis have been published elsewhere [5], and the present paper is a self-contained user's guide. For the derivation of these results the reader is referred to Ref. [5].

The method is explained using an example. In Sec. 2.0 the relevant variables are identified and the optimization philosophy is explained. In Sec. 3.0 a typical parabolic trough collector is described, and its material properties and operating conditions are identified. Sections 4.0 and 5.0 address the optimization of rim angle θ and of geometrical concentration ratio C . The operating efficiency of the collector is calculated in Sec. 6.0. The sensitivity of the optimization procedure to changes in operating conditions is discussed in Secs. 7.0 and 8.0--in Sec. 7.0 with regard to operating temperature and in Sec. 8.0 with regard to collector orientation (e.g., east-west axis or north-south axis). Fortunately, the optimum was found to be broad enough for a single collector to be operated with nearly optimal performance over a relatively wide range of temperatures and in several orientations. This conclusion permits significant cost savings through standardization.

SERIO 

SECTION 2.0

OPTIMIZATION PHILOSOPHY

The performance of any solar energy system improves if the collector efficiency is increased. Therefore, the efficiency of the collector should be maximized if such a step does not significantly increase the collector cost. The variables affecting collector efficiency fall into several groups:

- (1) operating conditions (insolation, tracking mode, operating temperature, flow rate);
- (2) properties of materials (reflectance, absorptance);
- (3) receiver type (absorber shape, evacuated or nonevacuated); and
- (4) concentrator geometry (concentration ratio C and rim angle θ).

Operating conditions may vary from installation to installation, but cost reduction by mass production requires some standardization of design. Thus, one would like to be able to design a solar collector that is approximately optimal for a range of operating conditions. The examples in this paper show that the optimum is indeed sufficiently broad to permit such standardization.

Initially, a generic receiver type (flat or cylindrical, evacuated or nonevacuated) is selected. For an evacuated receiver, a cylindrical absorber with a concentric glass envelope is probably the most reasonable choice, and the spacing between the absorber and glass envelope should be as small as is practical. For a nonevacuated receiver, the spacing between absorber surface and glazing should be as large as possible without initiating convection. If several candidate materials are available, the optimal choice is made by examining the cost and performance of each material.

Once the receiver type and materials are chosen, the concentrator geometry can be addressed. The geometric concentration ratio C is the ratio of the aperture area to the receiver surface area and is particularly important. As C is increased, the heat loss per aperture decreases, but the fraction of the incident solar radiation intercepted by the receiver also decreases. At the optimal concentration ratio, the incremental heat loss equals the incremental loss of intercepted solar radiation. Conceptually, it is more convenient to optimize the concentration ratio by fixing the receiver size and varying the aperture area. Only a single number, the heat loss rate q_L in W per m^2 receiver surface area, is needed to characterize the thermal properties of the receiver. The optimization is based on typical all-day average insolation data [16] rather than peak insolation at noon. For the optimization in this paper we assume a standard set of operating conditions (group 1) as a starting point and then choose different sets of values for the variables in groups 2 and 3. The concentration ratio and rim angle can then be optimized by the procedure developed in this paper. In practice, the mathematical optimum is not always the most desirable design because certain components (e.g., reflector sheets) may be available only in discrete sizes. Nonetheless, knowledge of the optimum is a valuable guide to the selection of a practical design.

SERIO 

SECTION 3.0

COLLECTOR PARAMETERS

Consider a long east-west mounted parabolic trough reflector (i.e., horizontal tracking axis aligned in the east-west direction) with a cylindrical receiver. The receiver has a selective coating and a glass envelope around it, as appropriate for operation in the 200°-300°C range [6]. The collector is characterized by the parameters listed in Table 1, which represent typical values for state-of-the-art technology. The contributions to beam spreading (σ , or optical error) are based on data reported by Sandia Laboratories for typical materials and fabrication techniques [7]. The reflectance ($\rho = 0.85$) is typical of clean aluminum or dirty silver reflectors. The transmittance τ and absorptance α are assumed to be 0.88 and 0.94, respectively, and are reasonable values when incidence angle effects are taken into account [8,9]. In practice the value of the reflectance-transmittance-absorptance product ($\rho\tau\alpha$) will be reduced by dirt, but compensating improvement with antireflection coatings is possible. Present operating experience is insufficient to evaluate with confidence the effects of long-term environmental degradation, but preliminary data [10,11] indicate that dirt on a reflector reduces the specular reflectance by about 0.05 to 0.2 (depending on the cleaning cycle) with little change in σ_{specular} . A value of 0.70 for the all-day average product $\langle(\rho\tau\alpha)\rangle$ appears to be realistic. In any case, only the product, not the individual factors, matters for the present purpose. At noon (normal incidence) it will be higher and $(\rho\tau\alpha)_{\text{normal}} = 0.73$ is assumed [8]; for more detailed data on the change in $(\rho\tau\alpha)$ with incidence angle, see Ref. 12.

Table 1. Collector Parameters

Parameter	Value
σ_{contourI}	2.5 mrad
$\sigma_{\text{contourII}}$	2.5 mrad
$\sigma_{\text{specularI}}$	2.0 mrad
$\sigma_{\text{specularII}}$	2.0 mrad
σ_{tracking}	2.0 mrad
$\sigma_{\text{displacement}}$	2.0 mrad
$\langle(\rho\tau\alpha)\rangle_{\text{EW}}$	0.70
$(\rho\tau\alpha)_{\text{normal}}$	0.73
d_{glass}	5.0 cm
d_{absorber}	2.5 cm
X_S	0.318
q_L	2000 W/m ²

In many concentrating collectors part of the aperture is shaded by the receiver. This effect can be accounted for by a shading correction (X_S in this paper). In the case of a cylindrical receiver with glazing, a comparable correction is needed for that fraction of the beam radiation incident on the aperture that passes between the glass and the receiver; due to refraction, this radiation deviates so much from the design direction that it misses the receiver altogether on its return from the reflector. To find a typical value of X_S for the configuration used as the example in this paper, we assume a receiver tube of 2.5-cm outer diameter (d_{absorber}), surrounded by a glass tube of 5-cm outer diameter (d_{glass}). (With reasonable glass thickness this leaves an air gap of 1.0 cm, which is approximately optimal in terms of heat transfer because the corresponding Rayleigh number is just below the onset of convection [18].) The shading correction is given by the formula

$$X_S = \frac{d_{\text{glass}} - d_{\text{absorber}}}{\pi d_{\text{absorber}}} \quad (\text{for cylindrical receiver with concentric glazing}) \quad (1a)$$

and has a value of 0.318 for this example (the factor of π is inserted for consistent normalization to absorber surface area). For a flat one-sided (i.e., back-insulated) absorber, X_S is given by

$$X_S = 1 + \frac{d_{\text{insulation}}}{d_{\text{absorber}}} \quad (\text{for flat absorber}) \quad , \quad (1b)$$

where $d_{\text{insulation}}$ is the total width by which the insulation extends beyond the absorber.

A crucial parameter is q_L , the heat loss rate per unit receiver surface area.* It must be interpreted as an average along the entire collector. All the thermal properties of the collector are included in this single parameter. For the purpose of this paper, only the value of this parameter is needed, while the detailed thermal properties are not of interest; in particular, the precise values of emissivity and heat extraction efficiency and the temperature nonuniformities are of no concern. For some important designs of cylindrical receivers we quote some results from Ref. 19 in Figs. 1(a)-(c). These figures show the heat loss coefficient based on absorber surface area,

$$U_L = \frac{q_L}{(T_{\text{abs}} - T_{\text{amb}}) A_{\text{abs}}} \quad ,$$

for a so-called "reference" receiver as well as for several receiver improvements. All of the receivers consist of a cylindrical absorber tube placed inside a concentric glass tube.

*The heat loss term q_L is defined with respect to receiver area rather than aperture area because in this optimization procedure for the concentration ratio the receiver area is fixed while the aperture is varied.

The reference receiver has an absorber tube diameter of 2.54 cm and a black chrome coating with an emittance of 0.15 at 100°C and 0.25 at 300°C, varying linearly between and beyond these limits. The receiver glazing has an emittance of 0.9. While the absorber tube diameter is fixed, the receiver glazing diameter is sized to minimize the conductive/convective losses. Too small a glass diameter (small gap) results in excessive conduction losses, whereas too large a glass diameter (large gap) results in excessive convection losses. The significance of the annulus gap size is shown in Fig. 1(a); the optimal gap size is seen to be around 0.7 cm, corresponding to an inner glass tube diameter of 3.9 cm.

Different absorber tube diameters will result in only slightly different heat loss coefficients U_L since U_L is based on absorber tube surface area, assuming, of course, that an optimal annulus gap size is chosen. Figure 1(b) illustrates this effect by showing the variation of U_L with receiver size. The variation is larger for the reference trough receiver than the evacuated receiver because conductive/convective losses do not increase directly with absorber diameter, while radiation losses nearly do. Larger-diameter absorbers result in smaller heat losses per unit absorber area. For an evacuated receiver the absorber diameter and gap have no effect on heat loss, and the gap should be as small as practical to minimize optical losses.

Figure 1(c) compares the heat loss coefficient of the reference receiver and several improved receivers as a function of temperature. The following improvements have been considered:

- emittance of absorber coating reduced to 0.05 at 100°C and 0.15 at 300°C (the reduced emittance is assumed linear between these limits);
- heat mirror coated receiver glazing with an emittance of 0.15;
- xenon back-filled annulus; and
- evacuated receiver.

The reader who is interested in calculating q_L is referred to the standard techniques described in the heat transfer literature.* If collector test data are available, we recommend taking for q_L the measured heat loss per unit of aperture area and multiplying by the geometric concentration ratio. Such data are reported in Ref. 6. The value $q_L = 2000 \text{ W/m}^2$ in Table 1 is typical for the collector serving as an example in this report.

*See, for example, Refs. 8, 9, or 13.

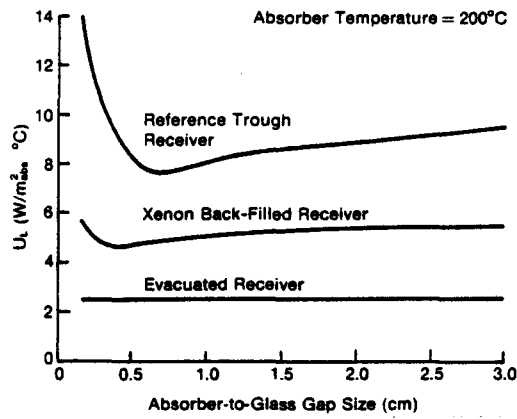


Figure 1a. Heat Loss Coefficient vs. Gap Size

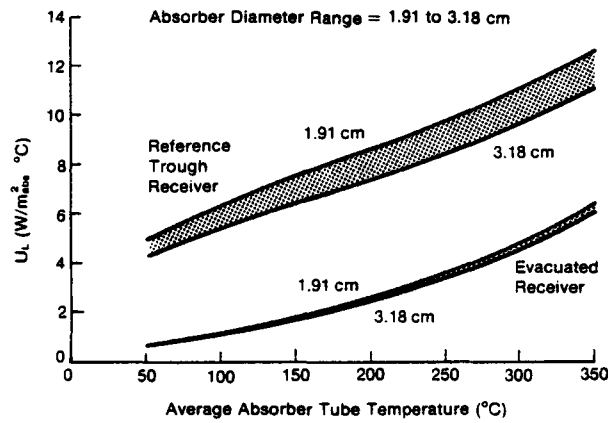


Figure 1b. Heat Loss Coefficient Variance with Absorber Diameter

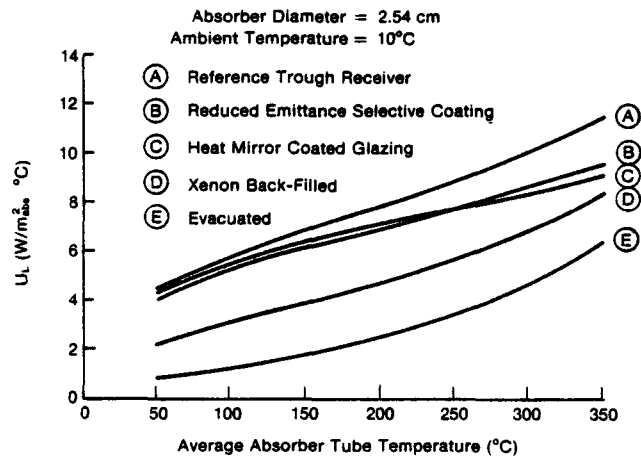


Figure 1c. Heat Loss Coefficient vs. Temperature

SOURCE: Ref. 19

SECTION 4.0

CHOICE OF RIM ANGLE

For cylindrical receivers the rim angle ϕ is in the range of 80 to 120 degrees, while for flat receivers it is in the range of 40 to 60 degrees. Figures 2(a) and 2(b) show the intercept factor γ (the fraction of incident radiation intercepted by the receiver) as a function of rim angle. A rim angle that maximizes the intercept factor should be chosen. However, Fig. 2 shows that γ is so close to its maximum over a broad range of values for ϕ that the choice of rim angle within this range can be determined by other considerations such as mechanical strength and ease of manufacture.

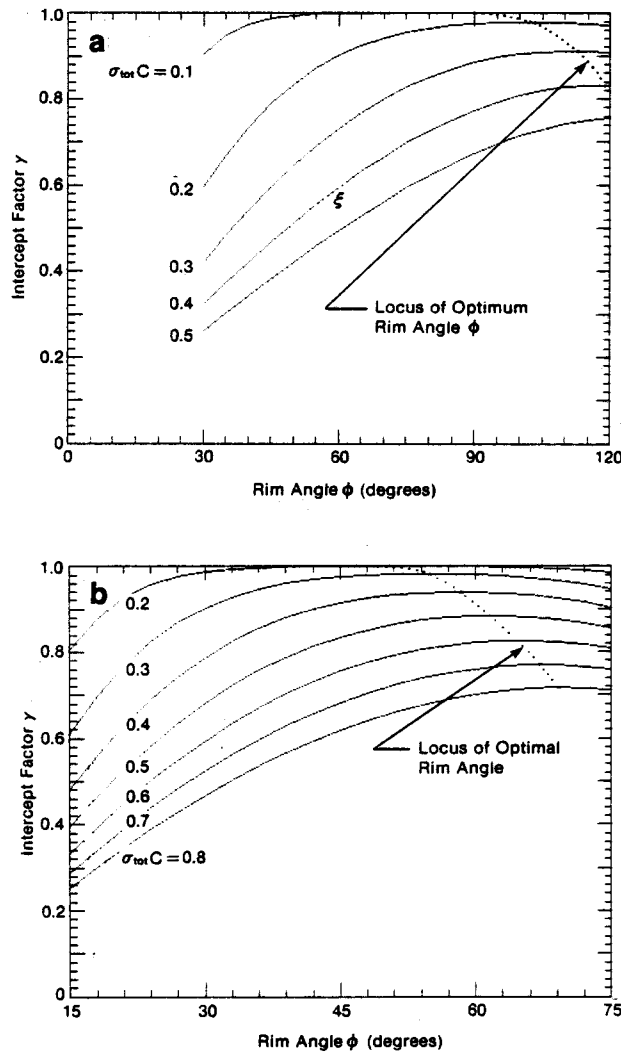


Figure 2. Intercept Factor γ vs. Rim Angle ϕ for Parabolic Trough (a) with Cylindrical Receiver (b) with Flat Receiver

SERIO 

SECTION 5.0

OPTIMIZATION OF CONCENTRATION RATIO

The appropriate insolation values for optimizing the concentration ratio with respect to all-day average performance depend on incidence angle and hence on tracking mode; values for the most important configurations are listed in Table 2. The all-day average quantities are designated by angular brackets and are based on an assumed operating time of 8 h/day. For other collection periods they can be recalculated by the methods presented in the appendix of Ref. 5.

Table 2. Tracking Modes and Associated Solar Data

Solar Data	Tracking Mode				
	E-W Axis Horizontal	N-S Axis Tilt-Latitude Polar	N-S Axis Horizontal at 35° N Latitude		
			Winter	Equinox	Summer
$\cos \theta_{\text{noon}}$	1.0	$\cos \delta$	0.52	0.82	0.98
$\sigma_{\text{sun,noon}}$ (mrad) ^a	4.1	4.3 ^e	7.9	5.0	4.2
$\langle \cos \theta \rangle$	0.77 ^b	0.96 ^e	0.63 ^b	0.89 ^c	0.99 ^d
$\langle \sigma_{\text{sun}} \rangle$ (mrad) ^a	5.0 ^b	4.3 ^e	6.6 ^b	4.6 ^c	4.2 ^d
$I_b \cos \theta_{\text{noon}}$ (W/m ²)	865.0	830.0 ^e	460.0	710.0	825.0
$\langle I_b \cos \theta \rangle$ (W/m ²)	665.0 ^b	750.0 ^{c,e}	490.0 ^b	670.0 ^c	720.0 ^d
$I_{d,\text{noon}}$ (W/m ²)	190.0	190.0	125.0	190.0	220.0
$\langle I_d \rangle$ (W/m ²)	160.0 ^b	140.0 ^c	95.0 ^b	140.0 ^c	160.0 ^d

^aAverage over typical sky conditions (circumsolar scans 1 through 10 in Table 4-1 of Ref. 5).

^bAll-day average based on 8 h/day.

^cAll-day average based on 10 h/day.

^dAll-day average based on 12 h/day.

^eIncludes all-year average of $\langle \cos \delta \rangle = 0.96$.

The steps of the calculation of the optimal concentration ratio C_o are listed in Table 3. First the optical error should be computed according to

$$\langle \sigma_{\text{optical}} \rangle^2 = 4 \sigma_{\text{contour}\perp}^2 + \sigma_{\text{specular}\perp}^2 + \lambda(\emptyset)(4 \sigma_{\text{contour}\parallel}^2 + \sigma_{\text{specular}\parallel}^2) + \sigma_{\text{tracking}}^2 + \sigma_{\text{displacement}}^2 \quad (2)$$

Table 3. Worksheet for Optimization of Concentration Ratio for Parabolic Trough with East-West Axis

Parameter	Value	Reference
$\lambda(\emptyset)$	0.1	Eq. 3b
$\langle \sigma_{\text{optical}} \rangle_{\text{EW}}$ (mrad)	6.3	Eqs. 2 and 4
$\langle \sigma_{\text{tot}} \rangle_{\text{EW}}$ (mrad)	8.0	Eq. 6
$\langle X \rangle_{\text{EW}}$	4.37	Eqs. 1 and 8
$\langle \sigma_{\text{tot}} \rangle_{\text{EW}} \langle X \rangle_{\text{EW}} = G(\langle \sigma_{\text{tot}} \rangle_{\text{EW}} C)$ (mrad)	35.0	Eq. 9
$\langle \sigma_{\text{tot}} \rangle_{\text{EW}} C_0$ (mrad)	218.0	Fig. 3a
C_0	27.3	Eq. 11

The coefficient $\lambda(\emptyset)$ represents the rim-angle-dependent contribution of longitudinal mirror errors to transverse beam spreading and depends weakly on incidence angle and hence on tracking mode. $\lambda(\emptyset)$ can be calculated from the equation

$$\lambda(\emptyset) = \langle n_x^2 \rangle_{\text{aperture}} \langle \tan^2 \theta_{\parallel} \rangle \tag{3a}$$

using values for $\langle n_x^2 \rangle_{\text{aperture}}$ and $\langle \tan^2 \theta_{\parallel} \rangle$ from Table 4. However, some simplification is permissible because λ is so small that its precise variation with \emptyset has negligible influence on the choice of optimal concentration ratio and rim angle. For the cases of greatest interest the following approximations can be used:

$$\lambda(\emptyset) = \begin{cases} 0 & \text{for normal incidence} \\ 0 & \text{for polar mount all-day average} \\ 0 & \text{for } \emptyset \lesssim 45^\circ \text{ for east-west tracking axis all-day average} \\ 0.1 & \text{for } 80^\circ \lesssim \emptyset \lesssim 110^\circ \text{ for east-west tracking axis all-day average} \end{cases} \tag{3b}$$

For our example the all-day average optical error is

$$\langle \sigma_{\text{optical}} \rangle_{\text{EW}}^2 = 1.1 \times (25 + 4) + 4 + 4 \text{ mrad}^2 = (6.3 \text{ mrad})^2 \tag{4}$$

To calculate the total rms beam spread $\langle \sigma_{\text{tot}} \rangle$, the value 4.1 mrad is used for the effective sun width $\sigma_{\text{sun,noon,average}}$, which is the average over circum-solar scans 1 through 10 (see Table 4-1 of Ref. 5). This appears to be representative of typical sky conditions and should be increased according to Eq. 5 to account for time-of-day variation:

$$\langle \sigma_{\text{sun}} \rangle_{\text{EW}} = \sqrt{1.5} \sigma_{\text{sun,noon,average}} = 5.0 \text{ mrad} \tag{5}$$

Table 4. Quantities Needed for Evaluation of Transverse Effects of Longitudinal Contour Errors in Parabolic Trough with East-West Tracking Axis

Average Over Aperture		Average Over Time of Day	
Rim Angle θ (degrees)	$\langle n_x^2 \rangle_{\text{aperture}}^a$	Cutoff Time t_c (h)	$\langle \tan^2 \theta_{\parallel} \rangle_{\text{day}}$
0	0.	0	0.0
30	0.023	3	0.2
45	0.052	4	0.5
60	0.093	5	0.9
75	0.147		
90	0.215		
105	0.297		
120	0.395		

$$^a \langle n_x^2 \rangle_{\text{aperture}} = 1 - \frac{0}{2 \tan^2(\theta/2)} .$$

The resulting total rms beam spread is

$$\langle \sigma_{\text{tot}} \rangle_{\text{EW}} = (\langle \sigma_{\text{optical}} \rangle_{\text{EW}}^2 + \langle \sigma_{\text{sun}} \rangle_{\text{EW}}^2)^{1/2} = 8.0 \text{ mrad} . \quad (6)$$

The average critical intensity ratio $\langle X \rangle$ is considered next:

$$\langle X \rangle = X_S + \left(\frac{q_L}{\langle (\rho \tau \alpha) \rangle} - \langle I_d \rangle \right) / \langle I_b \cos \theta \rangle . \quad (7)$$

When the data from Tables 1 and 2 are entered, we find

$$\langle X \rangle_{\text{EW}} = 0.318 + \left(\frac{2000}{0.70} - 160 \right) / 665 = 4.37 . \quad (8)$$

The curves $G(\sigma_{\text{tot}} C)$ of Figs. 3(a) and 3(b) can be used for finding the optimal concentration ratios C_o for different rim angles for cylindrical and flat receivers, respectively. A straight line drawn parallel to the abscissa ($\sigma_{\text{tot}} C$ axis) in Fig. 3(a) corresponding to the ordinate value

$$\langle \sigma_{\text{tot}} \rangle_{\text{EW}} \langle X \rangle_{\text{EW}} = 8.0 \times 4.37 \text{ mrad} = 35 \text{ mrad} \quad (9)$$

intersects the curve for $\theta = 90$ degrees at

$$\sigma_{\text{tot}} C = 218 \text{ mrad} . \quad (10)$$

This is the product of $\langle \sigma_{tot} \rangle_{EW}$ and the optimal concentration ratio C_o for this collector. Thus, the optimal concentration ratio which maximizes all-day efficiency is

$$C_o = \frac{218 \text{ mrad}}{8 \text{ mrad}} = 27.3 \quad (11)$$

The efficiency has a broad maximum at C_o ; therefore, a range of concentration values from 25 to 30 can be recommended for this collector. Note that in this paper the geometric concentration ratio is defined as the ratio of aperture area to receiver surface area. For a parabolic trough of aperture width D and absorber tube diameter d_{absorber} , the concentration ratio is

$$C = \frac{D}{\pi d_{\text{absorber}}} \quad (12)$$

For an absorber tube diameter $d_{\text{absorber}} = 2.5 \text{ cm}$, the optimal aperture width is

$$D = C_o \pi d_{\text{absorber}} = 27.3 \times \pi \times 2.5 \text{ cm} = 214 \text{ cm} \quad (13)$$

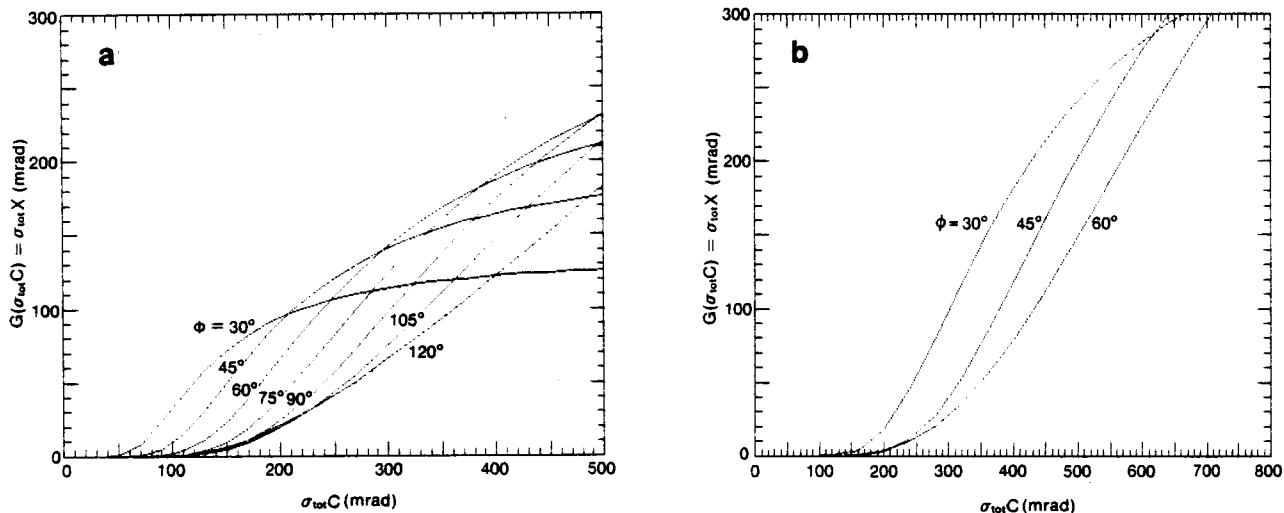


Figure 3. The Curve $G(\sigma_{tot} C)$ for Finding the Optimal Concentration Ratio for Different Rim Angles ϕ for (a) a Cylindrical Receiver (b) a Flat Receiver

SECTION 6.0

CALCULATION OF INTERCEPT FACTOR AND OPERATING EFFICIENCY

To calculate the operating efficiency it is important to know the intercept factor γ , which is defined as the fraction of those rays incident on the aperture that are intercepted by the receiver*:

$$\gamma = \frac{I_{in}}{I_b} \quad (14)$$

The intercept factor γ depends on $\sigma_{optical}$, sun shape, rim angle θ , and concentration ratio C . The calculation of γ can be greatly simplified if the sun shape can be approximated by a Gaussian brightness distribution. In this case, γ depends only on θ and on the product $\sigma_{tot} C$, where σ_{tot} is the total beam width of Eq. 6. The intercept factor can then be obtained from a single graph such as Figs. 4(a) and 4(b). As shown in Ref. 5, the errors resulting from this approximation are no greater than 1% for cases of practical interest; i.e., $C \lesssim 30$ and $\sigma_{optical} \gtrsim 5$ mrad.

In this section the efficiency

$$\eta = \frac{q_{net}}{I_b} \quad (15)$$

is calculated for peak and for all-day average conditions. The steps of the calculation are listed in the worksheet of Table 5. The efficiency can be expressed in terms of $(\rho\tau\alpha)$, γ , X , and C by

$$\eta = (\rho\tau\alpha) \left(\gamma - \frac{X}{C} \right) \quad (16)$$

The product $\eta_o = (\rho\tau\alpha) \gamma$ is the optical efficiency. To evaluate the all-day average operating efficiency $\langle \eta \rangle$, the parameters in Eq. 16 are based on the average sun shape and the average insolation level $\langle I_b \cos \theta \rangle_{EW} = 665 \text{ W/m}^2$, as in Sec. 5.0. With the resulting values

$$\langle (\rho\tau\alpha) \rangle_{EW} = 0.70,$$

$$\langle \gamma \rangle_{EW} = 0.965 \text{ [read from Fig. 4(a)} \\ \text{with } \langle \sigma_{tot} \rangle C = 218 \text{ mrad and } \theta = 90^\circ],$$

$$C_o = 27.3, \text{ and}$$

$$\langle X \rangle_{EW} = 4.37,$$

* γ is defined as a purely geometric quantity without regard to absorption or reflection losses.

Table 5. Worksheet for Calculation of Efficiency for Collector Optimized According to Table 3

Parameter	Value	Reference
C_o	27.3	Eq. 11
$\langle(\rho\tau\alpha)\rangle_{EW}$	0.70	Table 1
$\langle\sigma_{tot}\rangle_{EW} C_o$ (mrad)	218.0	Eq. 10
$\langle\gamma\rangle_{EW}$	0.965	Fig. 4a
$\langle X\rangle_{EW}$	4.37	Eq. 8
$\langle\eta\rangle_{EW}$	0.563	Eq. 17
$\sigma_{tot,noon}$ (mrad)	6.85	Eq. 18
$\sigma_{tot,noon} C_o$ (mrad)	187.0	--
γ_{noon}	0.982	Fig. 4a
X_{noon}	3.40	Eq. 19
$(\rho\tau\alpha)_{noon}$	0.73	Table 1
η_{noon}	0.63	Eq. 20

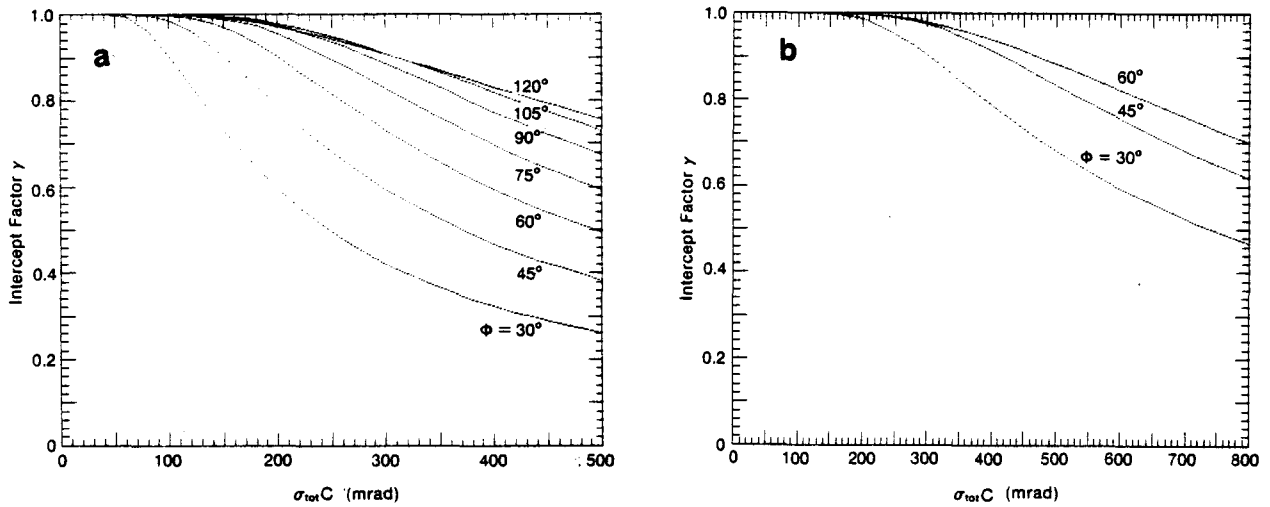


Figure 4. Intercept Factor γ vs. $\sigma_{tot} C$ for Different Rim Angles ϕ (Gaussian Approximation) for (a) a Cylindrical Receiver (b) a Flat Receiver

the average efficiency is*

$$\langle \eta \rangle_{EW} = \langle (\rho\tau\alpha) \rangle_{EW} \left(\langle \gamma \rangle_{EW} - \frac{\langle X \rangle_{EW}}{C_0} \right) = 0.563 \quad . \quad (17)$$

For extremely clear sky (narrow sun shape) and a typical peak insolation value $I_{b,peak}$ of 865 W/m^2 , the results for this collector are

$$\sigma_{\text{sun,narrow,noon}} = 2.7 \text{ mrad (from Table 4-1, data set \#1, of Ref. 5),}$$

$$\sigma_{\text{tot,noon}} = \left(\sigma_{\text{optical}}^2 + \sigma_{\text{sun,narrow,noon}}^2 \right)^{1/2} = 6.85 \text{ mrad,}$$

$$\gamma_{\text{noon}} = 0.982 \text{ [from Fig. 4(a)],} \quad (18)$$

and

$$X_{\text{noon}} = 0.318 + \left(\frac{2000}{0.7} - 191 \right) / 865 = 3.40 \quad . \quad (19)$$

The peak efficiency is thus

$$\eta_{\text{noon}} = (\rho\tau\alpha)_{\text{noon}} \left(\gamma_{\text{noon}} - \frac{X_{\text{noon}}}{C_0} \right) = 0.63 \quad . \quad (20)$$

This completes the calculations of optimal concentration ratio and of operating efficiency. Next we will consider the sensitivity of these results to changes in collector parameters and operating conditions.

*The only effect that has not been included is the spillover of radiation from collector ends in relatively short collectors. This end effect is installation-dependent and negligible for well-designed large collector fields. For short collectors (for example, test modules without end reflectors) this effect must be included by multiplying the intercept factor γ in Eq. 16 by an additional factor

$$\Gamma = 1 - \frac{f}{\lambda} \left(1 + \frac{D^2}{48f^2} \right) \tan \theta \quad ,$$

where f = focal length, λ = trough length, D = trough width, and θ = incidence angle. This is discussed in Ref. 12.

SERIO 

SECTION 7.0

SENSITIVITY OF OPTIMIZATION TO CHANGES IN COLLECTOR PARAMETERS

Once a collector has been optimized for operation at a certain temperature, the deviation from optimal performance at different temperatures can be calculated. In our example the concentration ratio was optimized for a heat loss parameter $q_L = 2000 \text{ W/m}^2$. The efficiency of this collector can then be calculated for lower and higher temperatures corresponding, for example, to $q_L = 1000 \text{ W/m}^2$ and $q_L = 3000 \text{ W/m}^2$.

These efficiencies based on the original optimization can be compared with those resulting from optimization for the new heat loss levels. Table 6 lists the respective efficiencies and concentration ratios calculated with the Gaussian approximation for several values of the beam spread σ_{tot} . The central column with $q_L = 2000 \text{ W/m}^2$ contains only one entry for each value of σ_{tot} in the form $\eta(C = \dots) = \dots$. For each of the other two heat loss levels the upper entry lists η for C as optimized at $q_L = 2000 \text{ W/m}^2$, and the lower line lists η with C' optimized for the new heat loss level.

Again the optimum range is rather broad. For example, if a concentrator with $\sigma_{tot} = 10 \text{ mrad}$ is optimized for operation at a temperature corresponding to a heat loss $q_L = 2000 \text{ W/m}^2$, it will perform with $\eta = 0.6109$ at half the heat loss. If the concentrator is optimized for operation at $q_L = 1000 \text{ W/m}^2$ the efficiency will be $\eta = 0.6156$, a gain of only 0.5%. This insensitivity to operating temperature eliminates the need to reoptimize for each new application and makes it possible to market a single collector for a fairly wide range of operating conditions.

Table 6. Sensitivity of Optimization to Change in Heat Loss Parameter q_L

σ_{tot} (mrad)	$q_L \text{ (W/m}^2\text{)}$		
	1000	2000	3000
5	$\eta(C = 37.92) = 0.6507$	$\eta(C = 37.92) = 0.6156$	$\eta(C = 37.92) = 0.5804$
	$\eta(C' = 33.15) = 0.6530$		$\eta(C' = 41.55) = 0.5820$
10	$\eta(C = 22.32) = 0.6109$	$\eta(C = 22.32) = 0.5511$	$\eta(C = 22.32) = 0.4913$
	$\eta(C' = 18.97) = 0.6156$		$\eta(C' = 25.01) = 0.4948$
20	$\eta(C = 13.75) = 0.5412$	$\eta(C = 13.75) = 0.4442$	$\eta(C = 13.75) = 0.3472$
	$\eta(C' = 11.17) = 0.5512$		$\eta(C' = 16.10) = 0.3547$

SERI 

SECTION 8.0

OPERATION WITH NORTH-SOUTH AXIS

Calculation of yearly energy delivery [14,15,17] shows that in midlatitudes (35 degrees) an aperture tracking about the horizontal north-south axis receives approximately 10% more energy than one tracking about the east-west axis. Polar axis tracking approaches within 4% the radiation availability of a two-axis tracker, surpassing the horizontal east-west axis by about 30%. Despite its higher collection potential, the polar axis mount generally is believed to be impractical for large installations because of problems with wind loading and plumbing. Polar mount may, however, be desirable for small installations with relatively short collector modules. Polar mount may also be preferred for photovoltaic applications.

The horizontal north-south axis suffers from large seasonal variation in output, resulting from variation not only of insolation but also of optical efficiency at low incidence angles. For a quantitative assessment of these effects, we evaluate the performance of the collector discussed in this paper if it is operated with a horizontal north-south instead of an east-west axis. The concentration ratio $C_o = 27.3$ is assumed as optimized for the collector with an east-west orientation. Table 7 lists the steps of the calculations for the winter and summer solstices and the equinox.

Table 7. Calculation of Efficiency of Collector with $C = 27.3$ (Optimized for East-West Axis) If Operated with Horizontal North-South Axis

Parameter	Value			Reference
	Winter	Equinox	Summer	
$\langle \rho\tau\alpha \rangle_{NS}$	0.70	0.73	0.73	Table 1
$\langle \sigma_{sun} \rangle_{NS}$ (mrad)	6.6	4.6	4.2	Table 2
$\lambda(\emptyset)$	0.34	0.06	0.0	Eq. 3
$\langle \sigma_{optical} \rangle_{NS}$ (mrad)	6.85	6.22	6.10	Eq. 2
$\langle \sigma_{tot} \rangle_{NS}$ (mrad)	9.51	7.75	7.38	Eq. 6
$\langle I_b \cos \theta \rangle_{NS}$ (W/m^2)	490.0	670.0	720.0	Table 2
$\langle I_d \rangle_{NS}$ (W/m^2)	95.0	140.0	160.0	Table 2
$\langle X \rangle_{NS}$	5.95	4.21	3.89	Eq. 7
$\langle \sigma_{tot} \rangle_{NS} C_o$ (mrad)	260.0	212.0	201.0	Fig. 3a
C_o	27.3	27.4	27.2	--
$\langle Y \rangle_{NS}$	0.926	0.966	0.971	Fig. 4a
$\langle \eta \rangle_{NS}$	0.50	0.59	0.61	Eq. 17

The second to the last line of Table 7 shows that the intercept factor varies little from 0.97 during spring and summer but drops to 0.926 at the winter solstice. This factor, coupled with a decreased $(\rho\alpha)$ product and lower beam insolation per aperture, leads to a significant drop in average operating efficiency from about 0.60 during the summer to 0.50 at the winter solstice. Whether such low efficiency is acceptable during a period of low available insolation depends on the load for each particular application. This situation does not change if the collector is optimized specifically for north-south orientation. If the optimization procedure described in Sec. 5.0 is repeated for the north-south orientation and for the summer and winter solstices and the equinox, the optimal concentration ratios differ very little: 27.3 for winter, 27.4 for equinox, and 27.2 for summer solstice. Thus, a single concentration ratio in the range of 25 to 30 is optimal for such a collector regardless of the orientation of the tracking axis.

SECTION 9.0

REFERENCES

1. Biggs, F.; Vittitoe, C. N. 1976. The Helios Model for the Optical Behavior of Reflecting Solar Concentrators. SAND 76-0347. Albuquerque, NM: Sandia Labs.
2. Schrenk, G. M. 1963 (Dec.). Analysis of Solar Reflectors: Mathematical Theory and Methodology for Simulation of Real Reflectors. GMC-AO-EDR3693.
3. Treadwell, G. W. 1976. Design Considerations for Parabolic Cylindrical Solar Collectors. SAND 76-0082. Albuquerque, NM: Sandia Labs.
4. Singh, P.; Cheema, L. S. 1976. "Performance and Optimization of a Cylindrical-Parabola Collector." Solar Energy. Vol. 18: p. 135.
5. Bendt, P.; Rabl, A.; Gaul, H. W.; Reed, K. A. 1979 (Sept.). Optical Analysis and Optimization of Line Focus Solar Collectors. SERI/TR-36-092. Golden, CO: Solar Energy Research Institute.
6. Dudley, V. E.; Workhoven, R. M. 1978 (May). Summary Report: Concentrating Solar Collector Test Results, Collector Module Test Facility. SAND 78-0815. Albuquerque, NM: Sandia Labs.
7. Butler, B. L.; Pettit, R. B. 1977. "Optical Evaluation Techniques for Reflecting Solar Concentrators." Vol. 114: Optics Applied to Solar Energy Conversion. Society of Photo-optical Instrumentation Engineers (SPIE). p. 43.
8. Duffie, J. A.; Beckman, W. A. 1974. Solar Energy Thermal Processes. New York, NY: John Wiley & Sons.
9. Kreith, F.; Kreider, J. F. 1978. Principles of Solar Engineering. New York, NY: McGraw-Hill.
10. Pettit, R. B.; Freese, J. M.; Arvizu, D. E. "Specular Reflectance Loss of Solar Mirrors due to Dirt Accumulation." Presented at IES Testing Solar Energy Materials and Systems Seminar; 22-26 May 1978. Washington, DC: National Bureau of Standards.
11. Freese, J. M. 1978. Effects of Outdoor Exposure on the Solar Reflectance Properties of Silvered Glass Mirrors. SAND 78-1649. Albuquerque, NM: Sandia Labs.
12. Gaul, H. W.; Rabl, A. 1980. "Incidence Angle Modifier and Average Optical Efficiency of Parabolic Trough Collectors." ASME Journal of Solar Energy Engineering. Vol. 102: p. 16.
13. Kreith, F. 1973. Principles of Heat Transfer. New York, NY: Intext Educational Publishers.

14. Dickinson, W. C. 1978. "Annual Available Radiation for Fixed and Tracking Collectors." Solar Energy. Vol. 21: p. 249.
15. Collares-Pereira, M.; Rabl, A. 1979. "Simple Procedure for Predicting Long-term Average Performance of Nonconcentrating and of Concentrating Solar Collectors." Solar Energy. Vol. 23: p. 235.
16. Collares-Pereira, M.; Rabl, A. 1979. "The Average Distribution of Solar Radiation: Correlations Between Diffuse and Hemispherical and Between Daily and Hourly Insolation Values." Solar Energy. Vol. 22: p. 155.
17. Rabl, A. 1980. "Yearly Average Performance of the Principal Solar Collector Types." SERI TP-631-716. To be published in Solar Energy.
18. Kreith, F. 1973. Principles of Heat Transfer. New York, NY: Intext Educational Publishers.
19. Gee, R., Gaul, H. W., Kearney, D., and Rabl, A. 1980. "Long Term Average Performance Benefits of Parabolic Trough Improvements." SERI/TR-632-439. Golden, CO: Solar Energy Research Institute.



National Renewable
Energy Laboratory



02LIB094340